NANO LETTERS

Letter

pubs.acs.org/NanoLett

# Gold Nanorods as Absorption Contrast Agents for the Noninvasive Detection of Arterial Vascular Disorders Based on Diffusion Reflection Measurements

Rinat Ankri,[†,§] Dorit Leshem-Lev,[‡,§] Dror Fixler,[*,†] Rachela Popovtzer,[†] Menachem Motiei,[†] Ran Kornowski,[‡] Edith Hochhauser,[‡] and Eli I. Lev[‡]

[†]Faculty of Engineering and Institute of Nanotechnology and Advanced Materials, Bar-Ilan University, Ramat-Gan, 5290002, Israel

[‡]Cardiac Research Laboratories at the Felsenstein Medical Research Center and the Cardiology Department, Rabin Medical Center, Petah-Tikva, Israel

*S* *Supporting Information*

**ABSTRACT:** In this study we report the use of gold nanorods (GNRs) as absorption contrast agents in the diffusion reflection (DR) method for the in vivo detection of atherosclerotic injury. The early detection and characterization of atherosclerotic vascular disease is considered to be one of the greatest medical challenges today. We show that macrophage cells, which are major components of unstable active atherosclerotic plaques, uptake gold nanoparticles, resulting in a change in the optical properties of tissue-like phantoms and a unique DR profile. In vivo DR measurements of rats that underwent injury of the carotid artery showed a clear difference between the DR profiles of the injured compared with healthy arteries. The results suggest that DR measurements following GNRs administration represent a potential novel method for the early detection of atherosclerotic vascular disease.

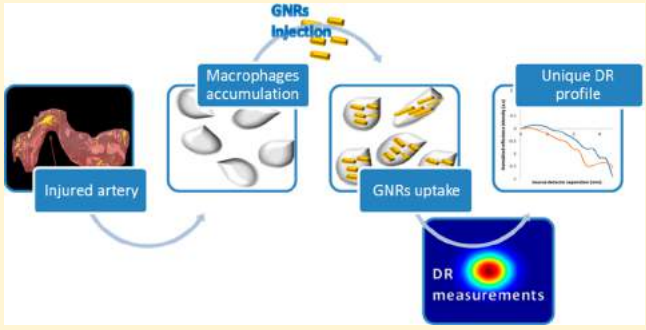


**KEYWORDS:** *Gold nanoparticles, gold nanorods, macrophages, biomolecular imaging, noninvasive detection*

Gold nanoparticles (GNPs) have long been used in the detection and imaging of biological processes and diseases.[1−4] The broad range of applications for GNPs is based on their unique chemical and physical properties and, in particular, on their optical properties from the visible to the infrared (IR) region, depending on the particle size, shape, and structure.[4−6] Diffusion reflection (DR) measurements of gold nanorods (GNRs) have been recently suggested as a new, simple, and very sensitive method for cancer detection.[7−9] The DR technique is based on a pair of source and detector fibers which are placed along the tissue surface, separated by distance origins from a few millimeters to a few centimeters, to enable the DR collection.[10,11] Once the GNPs accumulate in the specific tissue, the DR profile changes according to the optical properties of the GNPs. In the case of accumulated GNRs, the DR-GNRs method is based on the unique absorption properties of the GNRs which increase the absorption coefficient of the targeted site.

In this work, we extend our noninvasive DR-GNRs method to atherosclerotic vascular disease (ASVD) detection. Despite recent therapeutic advances, atherosclerosis and its major vascular complications—myocardial infarction and ischemic cerebrovascular accident—remain a leading cause of premature morbidity and mortality.[12−14] Over the last decades, noninvasive methods have been developed in order to detect atherosclerotic disease before it becomes symptomatic. These have included anatomical imaging techniques such as coronary calcium scoring by computed tomography (CT),[15,16] carotid intimal media thickness (IMT) measurement by ultrasound,[17,18] and magnetic resonance imaging (MRI).[19,20] The measurement of various biological markers is also available such as lipoprotein subclass analysis, hs-CRP, and other inflammatory marker levels.[21,22] Although there is a rapid progression in imaging techniques, the identification of early, inflamed "active" lesions within the coronary circulation remains elusive due to small plaque size, cardiac and respiratory motion, and lack of a suitable tracer/marker specific for the unstable plaque. The aim of this study is to develop a new, easy to use, and noninvasive method at low cost, to locate ASVD at its early stages. Anatomic detection methods are generally more expensive, and the physiologic methods do not quantify the current state of the disease accurately enough to track its progression.[23] Moreover, invasive methods, such as angiography, demonstrate changes in the lumen but not disease within the vessel wall. Therefore, the need for an improved detection method is of highly importance.

**Received:** February 13, 2014
**Revised:** March 25, 2014
**Published:** April 3, 2014

   dx.doi.org/10.1021/nl500573d | *Nano Lett.* 2014, 14, 2681−2687

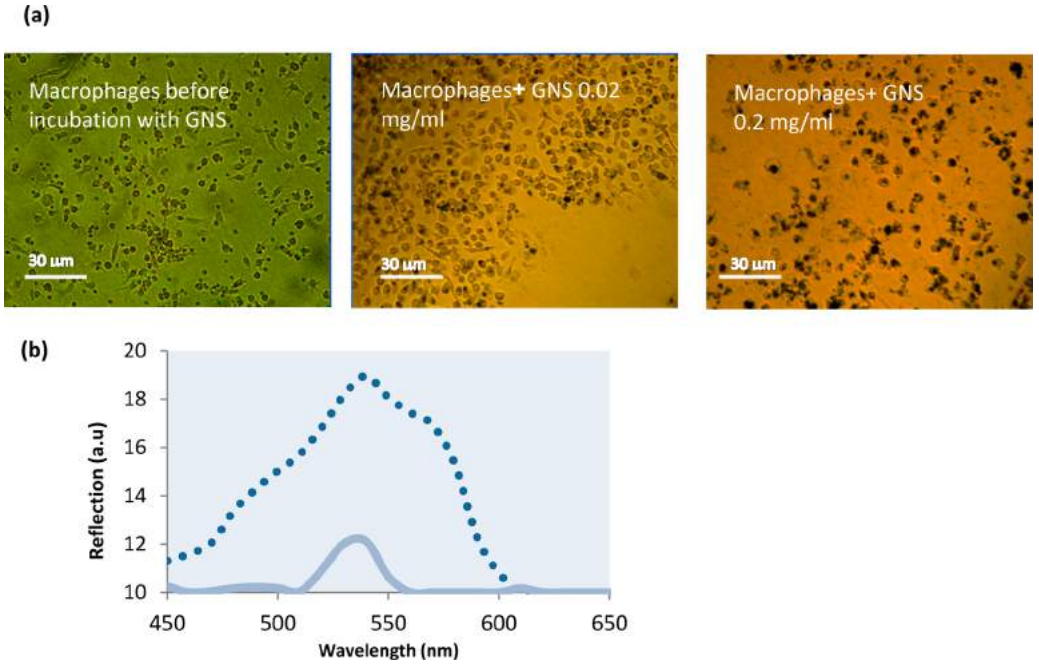


**Figure 1.** GNS uptake by macrophages captured by the hyper spectral microscopy. (a) Bright-field images of macrophages cells. Nanoparticles appear as dark dots within cells due to light absorption by the particles. (b) Reflectance intensity from macrophages 24 h after their incubation with 0.02 mg/mL (solid line) and 0.2 mg/mL (dotted line) of GNS. The spectra present an intensity peak at 540 nm, very much similar to the absorption peak of the GNS measured by the spectrophotometer (Figure S1a). The reflection spectrum of 0.2 mg/mL is broadened in comparsion to the reflectance spectrum of 0.02 mg/mL due to aggregation of highly concentrated GNS, resulting in an ensemble of red shifts.[28,29]

Accumulation of GNPs in an atherosclerotic active plaques is expected based on the known finding that phagocyte cells, including macrophages, can uptake metal nanoparticles[24,25] and since macrophages are major components of the unstable, inflammatory active atherosclerotic plaque.[26,27] Therefore, the combined DR of GNPs should present a new method to detect ASVD at its early stages. In this study we show that the DR method is able to detect, noninvasively, vascular disease following GNPs injection. We present GNPs uptake by the macrophages as was captured by a hyper spectral imaging system. DR measurements of tissue-like phantoms with macrophages, 24 h post GNPs injection, demonstrate in vitro that the DR method detects the 'golden' macrophages. In addition, in vivo DR measurements of carotid arteries in rats, as a model for atherosclerotic vascular diseases, are presented, showing a clear difference between the DR profiles of arteries following vascular injury vs control arteries. Ex vivo high-resolution CT measurements clearly prove the GNPs accumulation within the rat arteries, confirming the DR results. This article suggests, for the first time, a new, noninvasive method for the detection of atherosclerotic-like vascular disease.

The description of the gold nanospheres (GNS) and GNRs preparation and physical properties as well as the macrophages cells isolation are described in the Supporting Information (Materials and Methods section). The uptake of GNS by macrophages cells was verified using the hyper spectral microscopy. A primary human macrophage cell culture was incubated with 50 $\mu$L GNS (25 mg/mL) for 24 h at 37 °C. After incubation, the medium was washed twice with phosphate buffered saline, and the cells images were captured using the hyper spectral imaging system. Figure 1a presents pictures of the cells before and after their incubation with two different concentrations of GNS: 0.02 and 0.2 mg/mL. The cellular uptake of the GNS is clearly observed as dark dots that appear within the cells (dots are dark due to the absorption properties of the GNS). These in vitro experiments also demonstrate that the GNS uptake depends on their concentration: for the same amount of cells, the higher the GNS concentration, the more dark dots appear within the cells. Figure 1b shows the reflectance spectra of the macrophages after their incubation with the GNS. The spectra ensure the gold uptake by the macrophages, as they are very similar to the absorption spectrum of the GNS (Figure S1a). Moreover, the GNS uptake by the macrophages clearly depends on the GNS concentration: the higher the concentration, the higher the reflection intensity.

The next step was to insert macrophages into tissue-like phantoms, after their incubation with GNPs. Macrophages were incubated with GNRs (0.2 mg/mL) for 24 h, then were dissociated from the surface with Trypsin and solidified within the phantoms. The DR from the phantoms with and without macrophages was measured using our DR system. The phantoms were irradiated with 780 nm illumination, according to the absorption peak of the GNRs (Figure S1b). Four types of phantoms were measured: phantoms with GNRs (0.2 mg/mL), phantoms without GNRs, phantoms with macrophages, and phantoms with macrophages that were incubated for 24 h with GNRs (Figure 2a). The slope of each reflectance spectrum was extracted (the procedure for the slope extraction is detailed at Ankri et al., 2012),[8] and the average slopes are presented in Figure 2c (representative DR curves are presented in Figure 2b). It is well noted that the slopes resulting from the DR of phantoms with GNRs are very similar to those associated with the phantoms containing macrophages post GNRs incubation. These results indicate the GNRs uptake by the macrophages and, particularly, the DR method capability for detecting macrophages in tissue-like condition. It paved the way for in


dx.doi.org/10.1021/nl500573d | Nano Lett. 2014, 14, 2681−2687

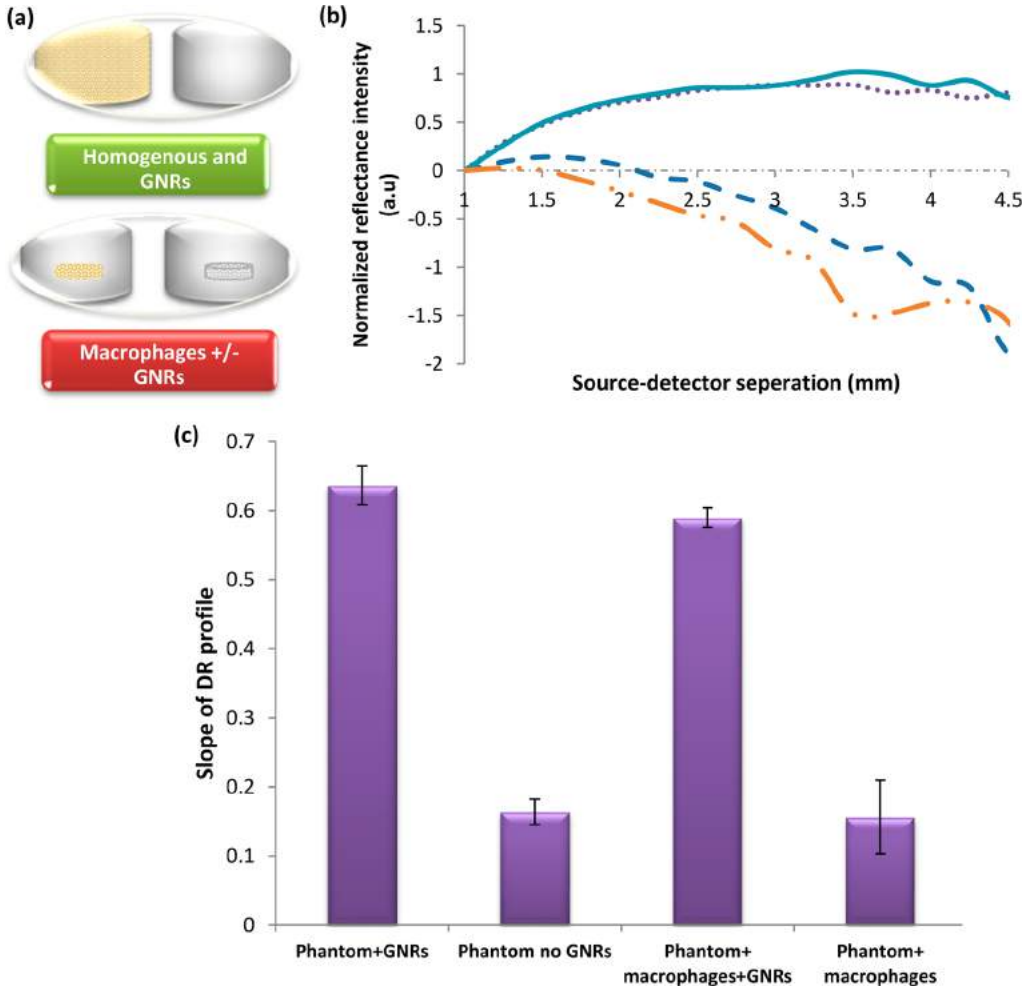


**Figure 2.** Diffusion reflection measurements of tissue-like phantoms. (a) Illustration of the two pairs of phantoms that were irradiated. Up: Phantoms with and without (homogeneous) GNRs. Bottom: Phantoms with macrophages before and after their incubation with GNRs. (b) Representative DR curves of the four types of phantoms: homogeneous (solid line), with 0.2 mg/mL of GNRs (dashed-dotted line), with macrophages before their incubation with GNRs (dotted line), and with macrophages after their incubation with 0.2 mg/mL GNRs (dashed line). (c) Averaged slopes resulting from the DR curves of the above-mentioned phantoms. The first and second columns represent phantoms with and without GNRs (0.2 mg/mL), respectively. The third, phantoms with macrophages following their 24 h incubation with 0.2 mg/mL GNRs. The fourth column represents phantoms with macrophages that were not incubated with GNRs. The slope of the phantoms with macrophages that were not incubated with GNRs was very similar to the phantom without GNRs, indicating that the macrophages presence within a tissue does not change the optical properties of the tissue.

vivo DR measurements of atherosclerotic vascular disease model in rats.

Atherosclerotic vascular disease model in rats was induced using carotid artery balloon injury.[30] Immunohistochemistry analyses were performed following the treatment to evaluate inflammatory cell accumulation (Figure S3). Rats were scanned in our DR system after a balloon injury of one of their carotid arteries. The injured artery was scanned noninvasively through the rat neck 24 h post the GNRs injection. Healthy carotid artery, located in the opposite side of the rat's neck, was also scanned and served as a control. In addition, we irradiated both the injured and the noninjured healthy arteries with 650 nm illumination, which is spectrally far from the injected GNRs absorption peak (see Figure S1b). Illustration of the spatial diffusion of light on the healthy and injured arteries surface is presented in Figure 3a: the diffusion of light decreases stronger in the injured artery due to the GNRs uptake by the macrophages, resulting in a higher absorption coefficient of the tissue. This theory is clearly demonstrated by the DR curves presented in Figure 3b: The reflection slope of the injured artery was about 5 times higher than the slope of the same artery before the GNRs injection as well as compared to the noninjured artery. These results suggest the DR method to be a highly sensitive detection method for ASVD.

Figure 4 presents a high-resolution CT image of the rat arteries 24 h post GNRs injection. GNRs along the arteries can be clearly identified as golden regions, since gold induces stronger X-ray attenuation.[31] Figure 4a shows the CT scan of the injured artery, distorted due to the balloon injury. In the injured region of the artery high concentrations of gold were accumulated. The gold accumulation in this region was likely due to the gold uptake by macrophages and other mononuclear cells, known to be recruited and to infiltrate the arterial vessel wall following injury.[32,33] Figure 4b depicts a CT image of the healthy noninjured artery, on the opposite side of the rat's neck. Presence of gold can still be observed but in significantly lower amounts. Importantly, no gold accumulation in a specific region was observed, suggesting that macrophages did not accumulate


dx.doi.org/10.1021/nl500573d | Nano Lett. 2014, 14, 2681−2687

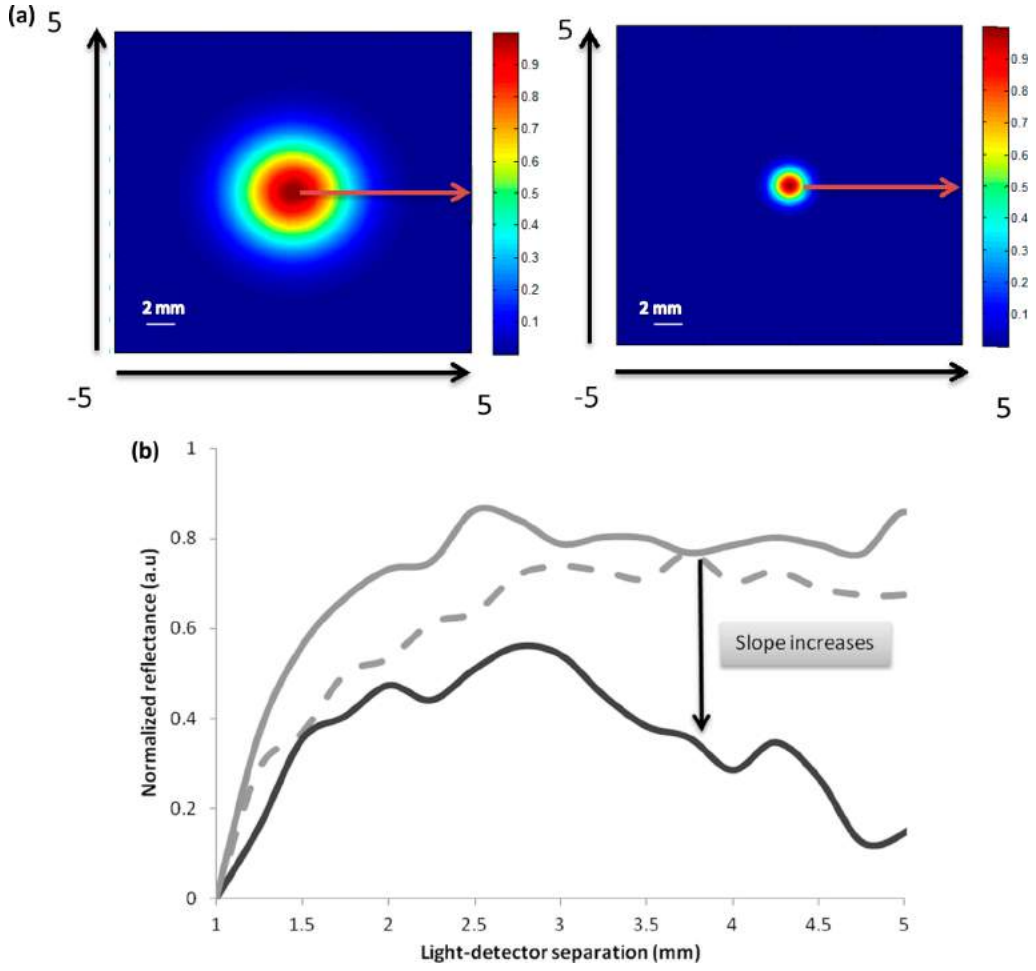


**Figure 3.** DR of a rat balloon-injured carotid artery. (a) Illustrative diffusion of light in the healthy (left panel) and injured (right panel) arteries. The illustration suggests that the intensity of light decreases stronger in the injured artery due to GNRs accumulation, which increases the absorption coefficient of the injured artery. The arrows present the light source-detector separations (in millimeters), indicating that reflection was measured from 1 to 5 mm. (b) Normalized diffusion reflection curves of a rat balloon-injured carotid artery measured by our DR technique. The dashed line represents the reflection from the injured artery before the GNRs injection. The solid dark line represents the reflection from the injured artery 24 h post GNRs injection and the solid light line the reflection from the noninjured healthy arteries (control). The slopes directly depend on the absorption coefficient of the tissue, correlated with the GNRs concentration within the tissue. Thus, the slope of the injured artery increased following the GNRs administration due to GNRs uptake by the macrophages. All curves are presented in the logarithmic form $\ln[\rho^2\Gamma(\rho)]$, since it enables the extraction of the GNRs concentration in the irradiated tissue (see Ankri et al, 2012).[8] The curve starts to decrease for $\rho > \sim 2$ mm since only from this point the decrease of $\Gamma(\rho)$ is more dominant than the increase of $\rho^2$.

in this artery. These CT images strengthen our diffusion reflection results, as both indicate accumulation of gold in the injured artery. In the Supporting Information, 3D and 4D videos show the differences between the GNRs spreading in the injured and the healthy arteries: While the GNRs in the injured artery were specifically concentrated in the artery's walls, in the healthy artery GNRs were homogeneously dispersed, indicating the absence of macrophages accumulation. Another important finding is that a regular in vivo CT scan does not reveal gold in the injured artery (Figure S4), while the DR method does reveal it under the same conditions.

The results presented in this paper support the need for a sensitive imaging method for the detection of vascular disease. ASVD is a chronic disease that remains asymptomatic for years.[34] Current imaging techniques are limited to detect early ASVD. Invasive techniques such as angiography have been widely employed to visualize the inside, or lumen, of blood vessels, with particular emphasis on the coronary arteries.[35] Another invasive technique is the intravascular ultrasound (IVUS) that provides cross-sectional images of blood vessels, having the ability to detect and characterize atherosclerotic plaque.[36,37] Noninvasive CT angiography can also detect significant narrowing and occluding processes in the lumens of various blood vessels. However, these methods focus on detecting significant luminal narrowing and to a lesser extent on characterizing the underlying ASVD disease. Our study presents a new potential biotechnology method for noninvasive detection of early ASVD.

The ASVD plaques are divided into two broad categories: stable and unstable (also called vulnerable plaques). Stable atherosclerotic plaques tend to be rich in extracellular matrices and smooth muscle cells, while unstable plaques are rich in macrophages, foam and inflammatory cells, and usually have a weak fibrous cap.[38] The unstable plaques are prone to rupture into the circulation, inducing thrombus formation in the lumen.[39] Therefore, their detection is critical. One of the most common and fatal complications of ASVD is ruptured unstable plaque followed by thrombotic occlusion, causing myocardial


dx.doi.org/10.1021/nl500573d | Nano Lett. 2014, 14, 2681−2687

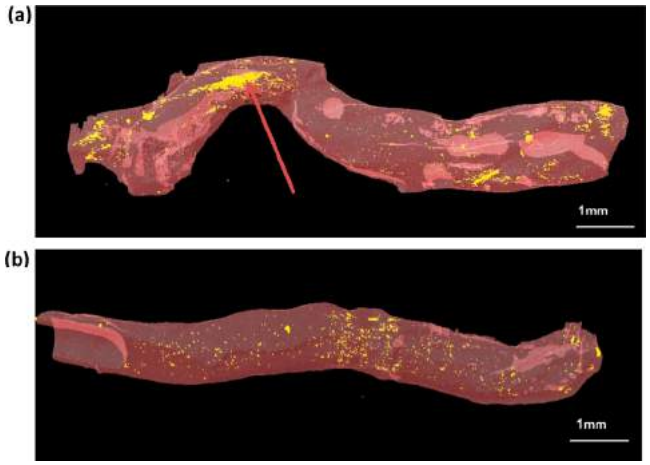


**Figure 4.** Ex vivo high-resolution CT scan of rat injured and healthy arteries. (a) The injured artery. The arrow indicates the distortion in the artery, caused by the injury. It is clearly evident that the GNRs were accumulated in the injured area, most probably due to accumulation within macrophages or in other mononuclear cells. (b) The healthy artery. A lower amount of GNRs was accumulated. In addition, the GNRs were homogeneously spread within the artery, rather than amassed in one area.

infarction. Meanwhile, there is no reliable method that can distinguish between these two kinds of plaques or detect unstable plaques, prone to rupture.[40,41] In this study we demonstrate the ability to specifically detect vascular areas with accumulation of macrophages cells, typical of unstable atherosclerotic plaques. The in vivo model for ASVD was based on a rat carotid artery balloon injury, in which macrophages and other mononuclear cells are recruited and infiltrate the arterial vessel wall following injury. The vascular injury area was specifically identified by GNRs uptake, presumably by macrophages.[42] Our results demonstrate the high efficiency of the DR method, using GNPs, in the detection of macrophages in vitro and in vascular areas following local injury in vivo. The high-resolution CT images as well as the histology prove that GNRs can accumulate within vessel walls, as in the injured artery's walls in the current study, causing a change in its optical properties and, thereby, a change in the DR profile of the irradiated tissue. It is important to note that in contrast to other imaging methods using GNPs, such as for cancer detection,[43,44] there is no need to bioconjugate the GNPs in the detection of ASVD, since the macrophages uptake pure GNPs. Moreover, the absorption properties of the GNRs are usually suggested for therapeutic purpose, such as photothermal therapy,[45] but, uniquely, the DR method presents the absorption properties of the GNPs to server as contrast agents for imaging purposes. Our previous studies show that the DR method detects even very small concentrations of GNRs.[8,29] Thus, small, early but inflammatory active atherosclerotic plaques can be detected in subjects with ASVD at its early stages by the DR method. The dependence of the ASVD stage and GNRs concentration on the detected signal should be further explored.

In conclusion, in this study we demonstrate that the DR method using GNPs is able to detect macrophage accumulation following vascular injury and, thus, may provide a promising novel detection tool for identification of early ASVD and unstable atherosclerotic plaques. Further investigation is required to use the GNPs as drug carriers for possible therapeutic applications.

## ■ ASSOCIATED CONTENT

### Ⓢ Supporting Information

Materials and methods, in vivo CT results, and supplementary videos. This material is available free of charge via the Internet at http://pubs.acs.org.

## ■ AUTHOR INFORMATION

### Corresponding Author

*E-mail: Dror.Fixler@biu.ac.il. Telephone: +972-3-5317598.

### Author Contributions

§These authors contributed equally.

### Notes

The authors declare no competing financial interest.

## ■ REFERENCES

(1) Popovtzer, R.; Agrawal, A.; Kotov, N. A.; Popovtzer, A.; Balter, J.; Carey, T. E.; Kopelman, R. Targeted gold nanoparticles enable molecular CT imaging of cancer. *Nano Lett.* **2008**, *8*, 4593−4596.

(2) Zhang, Q.; Iwakuma, N.; Sharma, P.; Moudgil, B. M.; Wu, C.; McNeill, J.; Jiang, H.; Grobmyer, S. R. Gold nanoparticles as a contrast agent for in vivo tumor imaging with photoacoustic tomography. *Nanotechnology* **2009**, *20*, 395102−39519.

(3) Robinson, T. J.; Welsher, K.; Tabakman, S. M.; Sherlock, S. P.; Wang, H.; Luong, R. High Performance In Vivo Near-IR (>1 μm) Imaging and Photothermal Cancer Therapy with Carbon Nanotubes. *Nano Res.* **2010**, *3*, 779−793.

(4) Fixler, D.; Zalevsky, Z. In Vivo Tumor Detection Using Polarization and Wavelength Reflection Characteristics of Gold Nanorods. *Nano Lett.* **2013**, *13* (12), 6292−6296.

(5) Eustis, S.; El-Sayed, M. A. Why gold nanoparticles are more precious than pretty gold: noble metal surface plasmon resonance and its enhancement of the radiative and nonradiative properties of nanocrystals of different shapes. *Chem. Soc. Rev.* **2006**, *35* (3), 209−217.

(6) Jain, P. K.; Lee, K. S.; El-Sayed, I. H.; El-Sayed, M. A. Calculated Absorption and Scattering Properties of Gold Nanoparticles of Different Size, Shape, and Composition: Applications in Biological Imaging and Biomedicine. *J. Phys. Chem. B* **2006**, *110*, 7238−7248.

(7) Ankri, R.; Peretz, V.; Motiei, M.; Popovtzer, R.; Fixler, D. A new method for cancer detection based on diffusion reflection measurements of targeted gold nanorods. *Int. J. Nanomed.* **2012**, *7*, 449−455.

(8) Ankri, R.; Duadi, H.; Motiei, M.; Fixler, D. In-vivo tumor detection using diffusion reflection measurements of targeted gold nanorods - a quantitative study. *J. Biophotonics* **2012**, *5* (3), 263−273.

(9) Ankri, R.; Taitelbaum, H.; Fixler, D. Reflected light intensity profile of two-layer tissues: phantom experiments. *J. Biomed. Opt.* **2011**, *16* (8), 3605694.

(10) Kienle, A.; Lilge, L.; Patterson, M. S.; Hibst, R.; Steiner, R.; Wilson, B. C. Spatially resolved absolute diffuse reflectance measurements for noninvasive determination of the optical scattering and absorption coefficients of biological tissue. *Appl. Opt.* **1996**, *35* (13), 2304−2314.

(11) Doornbos, R. M. P.; Lang, R.; Aalders, M. C.; Cross, F. W.; Sterenborg, H. J. C. M. The determination of in vivo human tissue optical properties and absolute chromophore concentrations using spatially resolved steady-state diffuse reflectance spectroscopy. *Phys. Med. Biol.* **1999**, *44* (4), 967−981.

(12) Ward, M. M. Premature morbidity from cardiovascular and cerebrovascular diseases in women with systemic lupus erythematosus. *Arthritis Rheum.* **1999**, *42* (2), 338−346.

(13) Asanuma, Y.; Oeser, A.; Shintani, A. K.; Turner, E.; Olsen, N.; Fazio, S.; Linton, M. F.; Raggi, P.; Stein, C. M. Premature Coronary-Artery Atherosclerosis in Systemic Lupus Erythematosus. *N. Engl. J. Med.* **2003**, *349* (25), 2407−2415.

(14) Bruce, I. N. 'Not only...but also': factors that contribute to accelerated atherosclerosis and premature coronary heart disease in systemic lupus erythematosus. *Rheumatology* **2005**, *44* (12), 1492−1502.
(15) Callister, T. Q.; Cooil, B.; Raya, S. P.; Lippolis, N. J.; Russo, D. J.; Raggi, P. Coronary artery disease: improved reproducibility of calcium scoring with an electron-beam CT volumetric method. *Radiology* **1998**, *208* (3), 807−814.
(16) Dewey, M.; Hamm, B. Cost effectiveness of coronary angiography and calcium scoring using CT and stress MRI for diagnosis of coronary artery disease. *Eur. Radiol.* **2007**, *17* (5), 1301−1309.
(17) Leonard, D.; Akhter, T.; Nordmark, G.; Rönnblom, L.; Naessen, T. Increased carotid intima thickness and decreased media thickness in premenopausal women with systemic lupus erythematosus: an investigation by non-invasive high-frequency ultrasound. *Scand. J. Rheumatol.* **2011**, *40* (4), 279−282.
(18) Touboul, P. J.; Hennerici, M. G.; Meairs, S.; Adams, H.; Amarenco, P.; Bornstein, N.; Csiba, L.; Desvarieux, M.; Ebrahim, S.; Hernandez Hernandez, R.; Jaff, M.; Kownator, S.; Naqvi, T.; Prati, P.; Rundek, T.; Sitzer, M.; Schminke, U.; Tardif, J. C.; Taylor, A.; Vicaut, E.; Woo, K. S. Mannheim Carotid Intima-Media Thickness and Plaque Consensus (2004−2006−2011). *Cerebrovasc. Dis.* **2012**, *34* (4), 290−296.
(19) Parmar, J. P.; Rogers, W. J.; Mugler, J. P.; Baskurt, E.; Altes, T. A.; Nandalur, K. R.; Stukenborg, G. J.; Phillips, C. D.; Hagspiel, K. D.; Matsumoto, A. H.; Dake, M. D.; Kramer, C. M. Magnetic Resonance Imaging of Carotid Atherosclerotic Plaque in Clinically Suspected Acute Transient Ischemic Attack and Acute Ischemic Stroke. *Circulation* **2010**, *122* (20), 2031−2038.
(20) Fayad, Z. A.; Mani, V.; Woodward, M.; Kallend, D.; Bansilal, S.; Pozza, J.; Burgess, T.; Fuster, V.; Rudd, J. H. F.; Tawakol, A.; Farkouh, M. E. Rationale and design of dal-PLAQUE: A study assessing efficacy and safety of dalcetrapib on progression or regression of atherosclerosis using magnetic resonance imaging and 18F-fluorodeoxyglucose positron emission tomography/computed tomography. *Am. Heart J.* **2011**, *162* (2), 214−221 e2.
(21) Corrado, E.; Rizzo, M.; Coppola, G.; Fattouch, K.; Novo, G.; Marturana, I.; Ferrara, F.; Novo, S. An update on the role of markers of inflammation in atherosclerosis. *J. Atheroscler. Thromb.* **2010**, *17* (1), 1−11.
(22) Kalogeropoulos, A.; Georgiopoulou, V.; Psaty, B. M.; Rodondi, N.; Smith, A. L.; Harrison, D. G.; Liu, Y.; Hoffmann, U.; Bauer, D. C.; Newman, A. B.; Kritchevsky, S. B.; Harris, T. B.; Butler, J. Inflammatory Markers and Incident Heart Failure Risk in Older AdultsThe Health ABC (Health, Aging, and Body Composition) Study. *J. Am. Coll. Cardiol.* **2010**, *55* (19), 2129−2137.
(23) Lerakis, S.; Synetos, A.; Toutouzas, K.; Vavuranakis, M.; Tsiamis, E.; C, S. Imaging of the vulnerable plaque:noninvasive and invasive technique. *Am. J. Med. Sci.* **2008**, *336*, 342−334.
(24) Carlson, C.; Hussain, S. M.; Schrand, A. M.; K. Braydich-Stolle, L.; Hess, K. L.; Jones, R. L.; Schlager, J. J. Unique Cellular Interaction of Silver Nanoparticles: Size-Dependent Generation of Reactive Oxygen Species. *J. Phys. Chem. B* **2008**, *112* (43), 13608−13619.
(25) Arnida; Janát-Amsbury, M. M.; Ray, A.; Peterson, C. M.; Ghandehari, H. Geometry and surface characteristics of gold nanoparticles influence their biodistribution and uptake by macrophages. *Eur. J. Pharm. Biopharm.* **2011**, *77* (3), 417−423.
(26) Lameijer, M. A.; Tang, J.; Nahrendorf, M.; Beelen, R. H. J.; Mulder, W. J. M. Monocytes and macrophages as nanomedicinal targets for improved diagnosis and treatment of disease. *Expert Rev. Mol. Diagn.* **2013**, *13* (6), 567−580.
(27) Plascencia-Villa, G.; Bahena, D.; Rodriguez, A. R.; Ponce, A.; Jose-Yacaman, M. Advanced microscopy of star-shaped gold nanoparticles and their adsorption-uptake by macrophages. *Metallomics* **2013**, *5* (3), 242−250.
(28) Mallidi, S.; Larson, T.; Tam, J.; Joshi, P. P.; Karpiouk, A.; Sokolov, K.; Emelianov, S. Multiwavelength Photoacoustic Imaging and Plasmon Resonance Coupling of Gold Nanoparticles for Selective Detection of Cancer. *Nano Lett.* **2009**, *9* (8), 2825−2831.
(29) Ankri, R.; Meiri, A.; Lau, S. I.; Motiei, M.; Popovtzer, R.; Fixler, D. Intercoupling surface plasmon resonance and diffusion reflection measurements for real-time cancer detection. *J. Biophotonics* **2013**, *6* (2), 188−196.
(30) Tulis, D. A. Rat carotid artery balloon injury model. *Methods Mol. Med.* **2007**, *139*, 1−30.
(31) Sherman, A. I.; Ter-Pogossian, M. Lymph-node concentration of radioactive colloidal gold following interstitial injection. *Cancer* **1953**, *6* (6), 1238−1240.
(32) Simon, D. I. Inflammation and vascular injury: basic discovery to drug development. *Circ J.* **2012**, *76* (8), 1811−1818.
(33) Rogers, C.; Welt, F. G.; Karnovsky, M. J.; Edelman, E. R. Monocyte recruitment and neointimal hyperplasia in rabbits. Coupled inhibitory effects of heparin. *Arterioscler. Thromb. Vasc. Biol.* **1996**, *16* (10), 1312−1318.
(34) Yu, X.-H.; Fu, Y.-C.; Zhang, D.-W.; Yin, K.; Tang, C.-K. Foam cells in atherosclerosis. *Clin. Chim. Acta* **2013**, *424*, 245−252.
(35) Maddux, J. T.; Wink, O.; Messenger, J. C.; Groves, B. M.; Liao, R.; Strzelczyk, J.; Chen, S.-Y.; Carroll, J. D. Randomized study of the safety and clinical utility of rotational angiography versus standard angiography in the diagnosis of coronary artery disease. *Catheterization Cardiovasc. Interventions* **2004**, *62* (2), 167−174.
(36) Kotani, J.-i.; Mintz, G. S.; Castagna, M. T.; Pinnow, E.; Berzingi, C. O.; Bui, A. B.; Pichard, A. D.; Satler, L. F.; Suddath, W. O.; Waksman, R.; Laird, J. R.; Kent, K. M.; Weissman, N. J. Intravascular Ultrasound Analysis of Infarct-Related and Non−Infarct-Related Arteries in Patients Who Presented With an Acute Myocardial Infarction. *Circulation* **2003**, *107* (23), 2889−2893.
(37) Ehara, S.; Kobayashi, Y.; Yoshiyama, M.; Shimada, K.; Shimada, Y.; Fukuda, D.; Nakamura, Y.; Yamashita, H.; Yamagishi, H.; Takeuchi, K.; Naruko, T.; Haze, K.; Becker, A. E.; Yoshikawa, J.; Ueda, M. Spotty Calcification Typifies the Culprit Plaque in Patients With Acute Myocardial Infarction: An Intravascular Ultrasound Study. *Circulation* **2004**, *110* (22), 3424−3429.
(38) Davies, M. J. Stability and Instability: Two Faces of Coronary Atherosclerosis: The Paul Dudley White Lecture 1995. *Circulation* **1996**, *94* (8), 2013−2020.
(39) Fuster, V.; Stein, B.; Ambrose, J. A.; Badimon, L.; Badimon, J. J.; Chesebro, J. H. Atherosclerotic plaque rupture and thrombosis. Evolving concepts. *Circulation* **1990**, *82* (3 Suppl), II47−59.
(40) Jang, I.-K.; Bouma, B. E.; Kang, D.-H.; Park, S.-J.; Park, S.-W.; Seung, K.-B.; Choi, K.-B.; Shishkov, M.; Schlendorf, K.; Pomerantsev, E.; Houser, S. L.; Aretz, H. T.; Tearney, G. J. Visualization of coronary atherosclerotic plaques in patients using optical coherence tomography: comparison with intravascular ultrasound. *J. Am. Coll. Cardiol.* **2002**, *39* (4), 604−609.
(41) Stone, G. W.; Maehara, A.; Lansky, A. J.; de Bruyne, B.; Cristea, E.; Mintz, G. S.; Mehran, R.; McPherson, J.; Farhat, N.; Marso, S. P.; Parise, H.; Templin, B.; White, R.; Zhang, Z.; Serruys, P. W. A Prospective Natural-History Study of Coronary Atherosclerosis. *N. Engl. J. Med.* **2011**, *364* (3), 226−235.
(42) Afergan, E.; Ben David, M.; Epstein, H.; Koroukhov, N.; Gilhar, D.; Rohekar, K.; Danenberg, H.; Golomb, G. Liposomal Simvastatin Attenuates Neointimal Hyperplasia in Rats. *AAPS J.* **2010**, *12* (2), 181−187.
(43) Mieszawska, A. J.; Mulder, W. J. M.; Fayad, Z. A.; Cormode, D. P. Multifunctional Gold Nanoparticles for Diagnosis and Therapy of Disease. *Mol. Pharmaceutics* **2013**, *10* (3), 831−847.
(44) Eissa, S.; Shawky, S. M.; Matboli, M.; Mohamed, S.; Azzazy, H. M. E. Direct detection of unamplified hepatoma upregulated protein RNA in urine using gold nanoparticles for bladder cancer diagnosis. *Clin. Biochem.* **2014**, *47* (1−2), 104−110.
(45) Dickerson, E. B.; Dreaden, E. C.; Huang, X.; El-Sayed, I. H.; Chu, H.; Pushpanketh, S.; McDonald, J. F.; El-Sayed, M. A. Gold nanorod assisted near-infrared plasmonic photothermal therapy (PPTT) of squamous cell carcinoma in mice. *Cancer Lett.* **2008**, *269* (1), 57−66.

(46) Dickerson, E. B.; Dreaden, E. C.; Huang, X.; El-Sayed, I. H.; Chu, H.; Pushpanketh, S.; McDonald, J. F.; El-Sayed, M. A. Gold nanorod assisted near-infrared plasmonic photothermal therapy (PPTT) of squamous cell carcinoma in mice. *Cancer Lett.* **2008**, *269* (1), 57−66.